Improvement of Oncolytic Viral Therapy Through Transgenic Delivery of Constitutively Active EPAC

Bailey Organ

A Dissertation submitted to the University of Ottawa

Graduate Program of the Faculty of Medicine in Fulfillment of the Requirements for the Degree of Masters of Biochemistry with a Speciality in Human and Molecular Genetics

Master of Science

Department of Biochemistry, Microbiology & Immunology

Faculty Of Medicine

University of Ottawa

Supervisor: Dr. John C. Bell

Acknowledgments

First of all, I would like to thank my supervisor Dr. John Bell for his support and encouragement, and Dr. Carolina Ilkow for being a mentor and providing words of wisdom throughout my time here in the lab. I would also like to thank Dr. Stephen Boulton for his continued guidance and enthusiasm for the project over the past couple years, I am truly grateful to have been able to work with you closely. To Julia Petryk, I thank you for being the best lab manager, providing lots of laughs, being a great friend and for injecting 100's of mice for me over my time here. To the lab, Jaahnavi, Mathieu, Nikolas, Sarah, Jack Rida and Hanna thank you for the amazing work environment, daily brainstorming and weekend outings. Finally, a huge heartfelt appreciation to my family for supporting me very step of the way with endless love and support.

Abstract

Oncolytic viruses (OVs) are designed to selectively infect and kill cancer cells, while also initiating any anti-tumor immunity. They can be engineered to express therapeutic transgenes that improve their ability to spread through the tumor microenvironment or improve their oncolytic activity. In this thesis, I develop a collection of Vaccinia OVs that express the exchange protein activated by cAMP (EPAC) as a therapeutic payload to enhance virus spread in tumours. I show that poxviruses expressing constitutively active forms of EPAC improve viral spread *in vitro* in both cellular monolayers, Transwell assays and 3D tumour spheroids. In addition, the EPAC viruses decrease tumour growth and increase survival in mice with MC38 tumours. We also explore the combination of these viruses with the EPAC inhibitor ESI-09, which has anti-metastatic properties and which we show can inhibit B16 metastasis to the lungs following surgery resection. Our study shows that the Vaccinia virus expressing active EPAC shows promise as a potential cancer therapeutic.

Table of Contents

List of Figures

List of Abbreviations

AKT	Protein Kinase B
cAMP	Cyclic adenosine monophosphate
CR	Catalytic Region (of EPAC)
CTLA-4	Cytotoxic T lymphocyte Associated Protein 4
DNA	Deoxyribonucleic acid
DPI	Days Post Infection
EPAC	Exchange Protein activated by cAMP
FRET	Fluorescence resonance energy transfer
HPI	Hours Post Infection
HSV	Herpes Simplex Virus
IFN	Type 1 interferon
IL-10	Interleukin 10
IP	Interpretational
IT	Inter-tumour
M	Matrix Protein (of VSV)
mTOR	Rapamycin signaling
NOD/SCID	Mice homozygous for the severe combined immune deficiency spontaneous mutation $Prkdc^{scid}$
PD-L1	Protein Death Ligand 1
PDA	Pancreatic ductal adenocarcinoma

PKA	Protein Kinase A
RNA	Ribonucleic acid
RR	Regulatory Region (of EPAC)
SKV	Superior Killing Virus
TK	Thymidine Kinase
TT	Tiantan Virus
VACV	Vaccinia Virus
VSV	Vesicular Stomatitis Virus

1. ***Introduction***

Cancer, described as the uncontrolled division of cells in the body, is one of the leading cause of death in Canada. Despite the ongoing progress and treatment breakthroughs, cancer deaths continue to rise in Canada and across the world. While some forms of cancer cause many noticeable side effects that lead to early diagnosis, many go un-detected until the patient becomes severely unwell. Once cancer forms metastatic foci and begins to invade neighbouring cells and tissues, the effectiveness of current treatments decline, as well as patient quality of life. [1]

1. 2 Heterogeneity of Cancer

Cancer is a multi-faceted disease. Malignant tumours are composed of cells that have gained the ability to sustain chronic proliferation and enable replicative immortality, overriding systems set in place to prevent such actions, e.g. tumour suppressors and oncogenes. As a tumour progresses throughout the course of the disease its heterogeneity usually increases. [2] This means that the tumour may not express the same genetically distinct markers across tumour cell-subpopulations, or tumour disease sites, rendering most current drug therapies less and less effective against the tumour and ultimately leading to drug resistance. Cancer is a disease of genomic disfunction, meaning as cells divide, they are gaining or loosing functions that are not phenotypically normal to the host. [3] A variety of specific treatments are needed to target these signalling pathways that have been altered by pathogenic tumour cells.

1.3 Oncolytic viruses

1.3..1 Viral infection causes decrease in tumor burden

Oncolytic viruses (OVs) have emerged as a promising therapeutic in the fight against cancer. Oncolytic virotherapy is a form of immunotherapy that use replication-competent, non-

pathogenic viruses to selectively target and kill cancer cells. [4] Despite the only recent explosion in OV development and clinical trials for cancer, the observation that viral infections can lead to tumour regression dates back to the mid 1800's. [5] One of the most relevant documented charts in OV history involved a 42-year-old-women who went into remission from myelogenous leukemia after a presumed influenza infection in 1986. Similarly reported was the case of a young boy suffering from lymphatic leukemia who went into remission after contracting chickenpox. In both causes their livers and spleens were reported to be enormously oversized and within a few days of developing symptoms of viral infection, both livers returned to a normal healthy size. While remission was only for a few months it was ascertained that viral infection decreased tumour burden in patients with hematological malignancies.

Science first began to understand this phenomenon in the 1950's when research in viruses advanced. At this time, ex-vivo virus propagation in cell and tissue culture began and viruses were injected into cancer models which resulted in therapeutic activity. [4,5] Viruses studied at this time include: West Nile virus, Adenovirus and Urabe Strain Mumps virus. However, tumour selectivity was not specific, and patients often got sick after receiving viral strains. Fast forward to present day, commercial OVs are now available due to advances in genetic engineering that are tumour specific and have reduced side effects for the patient.

1.3.2 FDA Approved OV's

OV therapy has now been accepted as an anti-cancer agent in Canada. It has been observed that some viruses have an affinity for cancer cells while others can be genetically engineered to have the tropism for various pathways expressed in common cancers. To date, T-VEC a modified herpes simplex virus (HSV) has been approved for treatment for patients with melanoma. While T-VEC is the only OV currently approved in Canada, Japan has recently approved Teserpaturev,

a new oncolytic HSV virus for treatment against malignant glioma. Currently there are 54 ongoing clinical trials using oncolytic viruses. [6,7]

Oncolytic virotherapy research is not limited to HSV. There are many families of viruses being explored in both research and clinical studies today. Such viruses include: *Adenoviridae, Picornaviridae, Paramyxoviridae, Parvoviridae, Reoviridae, Poxviridae, Rhabdoviridae* and *Retroviridae*.[8]

1.4 Mechanisms of OV's

Tumor's lack some signaling pathways that viruses can specifically target

Tumors can progress and thrive in patients largely because neoplastic cells are able to evade the host immune system. One common mechanism of tumor evasion is the cancer cells ability to present MHC incorrectly allowing the cell to evade T-cell response.[3] Alternatively, another method of invasion includes the abnormal stimulation of the immune checkpoint creating an immunosuppressive environment. PD-L1 and CTLA-4 are examples of this phenomenon. When tumor cells express these receptors, antigen presenting T-cells are bound, keeping T-cells in an inactive state. Finally, tumors may evade immune responses by taking advantage of negative feedback mechanisms such as IL-10 that the body has in place to prevent immunopathology.[9] In addition to evading cellular defenses, tumors have evolved to thrive on the excess production of tumor associated macrophages. These macrophages mimic the evasive features of type M2 macrophages which have healthy bodily functions, such as tissue repair and pro- inflammatory responses. However, unlike M2 macrophages, tumor associated macrophages have anti-inflammatory properties which enables tumor progression and lacks tissue repair mechanisms.[10]

Understanding the methods of immune invasion and the natural tropism for viruses to target tumor environments, has laid the foundation for therapeutic responses. Further virus modifications and current research has allowed for pathway/protein specific targeting. As mentioned earlier, different tumors have common cancer drivers and common mutations that lead to the progression of the disease in patients.[3] Understanding these pathways has allowed for researchers to develop therapeutics by genetically modifying viruses, via additions or deletions of the viral genome.

Similar to tumor cells, Vesicular stomatitis virus (VSV) has a matrix protein (M) that plays a vital role in immune evasion. The viral protein is able to suppress production of Type 1 interferon (IFN), which under normal circumstances, inhibits viral reproduction. Therefore, scientists proposed using a mutated version of the M protein (referred to as VSVdelta51) that allows for VSV to be more susceptible to interferon by rendering the virus incapable of mitigating the patients antiviral response in healthy cells. The mutant VSVdelta51 can no longer block nuclear transport of mRNA's that are required for the production of IFN, therefore, limiting the propagation of viral particles to tumor cells. [11]

Another well-known virus modification to increase tumor selectivity is the thymidine kinase (TK) gene knockout in vaccinia. This knockout attempts to limit viral replication to just cancer tissues. While knocking out this pathway attenuates the virus, there are still other tissues that can overcome the lack of viral TK. Consequently, more studies are in progress to improve vaccinia as an oncolytic. [12]

1.5 Oncolytic Vaccinia virus

Vaccina virus (VACV) is a part of the genus Orthopoxvirus and of the family Poxiviridae. VACV and other closely related poxviruses have been used for centuries in the smallpox vaccination campaign. With VACV's impressive safety profile and its immunologic cross-

reactivity allowed for its use as a vaccine vector. VACV has a linear double stranded DNA genome, approximately. 200kb in length that encodes 209 genes: 118 early, 53 intermediate and 38 late genes.[13] Due to the nature of its size, the virus can be modified to incorporate large amounts of foreign DNA called transgenes. There are two infectious virus particle types; the mature and the wrapped virion. What makes this virus unique, and preferential for further study is the fact that unlike other DNA viruses, VACV's DNA replication occurs in the cytoplasm, so it is unlikely to integrate into the host's genome. The mature virus particle type always remains in the cytoplasm until cell lysis, whereas the wrapped particle type requires an additional two membranes from the endosomal network before exiting the cell via membrane fusion.[14]

1.5.1 SKV

Using bioengineering the Bell Lab developed a novel vaccina platform termed SKV (patent 9 , 896 , 664 B2). This engineered virus has 30 genes amounting to approximately 25 kb of the viral genome deleted on either end of the genome. These genes are virulence genes that antagonize the host, but are not required for viral replication. There are several noted advantages of the SKV strain over other non-attenuated oncolytic vaccinia viruses. First, the removal of 25kb of viral DNA opens up space to insert more foreign DNA in the form of therapeutic transgenes, meaning that SKV is a more versatile strategy for payload delivery to tumors. Second, since many of the deleted genes from SKV are modulatory genes that inhibit immune responses, the virus is much more susceptible to immune responses generated in healthy tissues. As such, its safety profile is markedly improved. This is best demonstrated by the fact that SKV, when administered systemically in immune deficient NOD/SCID mice, does not replicate in any tissues other than the tumor. Third, the deletion of immunomodulatory genes from SKV leads to better activation of interferon signaling genes in the tumor, resulting in better immune recruitment and activation. This

makes it better at generating anti-tumor immune responses. It also allows it to work synergistically with other immunotherapies such as immune checkpoint inhibitors. Lastly, the deletion of the K2L gene results in syncytia formation (cell fusion) in infected cells, which is good for inducing apoptosis in cancer cells.[15]

1.5.2 Transgenes

OVs have shown tremendous progress in recent years for treating various malignancies, their performance in clinical trials is still underwhelming, so there is a need to identify novel transgenes that can increase OV efficacy. Some common transgene strategies to date include, cytokines and immune checkpoint inhibitors such as anti-PD-1 and anti-CTLA-4 which can improve T cell expansion/persistence and allow activation of T-cells by blocking tumour presenting ligand binding.[16]

1.6 The exchange protein activated by cAMP (EPAC)

EPAC is cellular receptor for cyclic AMP (cAMP), a universal secondary messenger that regulates "flight or fight" responses in the body. On the cellular level, cAMP regulates a plethora of signaling pathways involved in everything from cell growth, metabolism and proliferation to neuronal rhythmicity. Until the late 1990s, many of the cellular pathways regulated by cAMP were attributed to its activation of protein kinase A (PKA), but once EPAC was identified as a cAMP receptor, it role in cell signaling was dissected from PKA's, showing that it had a unique signaling phenotype that sometimes complemented and other times antagonized that of PKA.[17]

EPAC serves as a guanine nucleotide exchange factor (GEF) for the small RAS-like GTPases, RAP1 and RAP2. The Rap proteins consequently regulate many downstream processes that are important for cell adhesion and cytoskeleton remodeling, exocytosis and secretion, endothelial barrier junctions and lastly cardiac functions. EPAC is also responsible for activating

the protein kinase B (Akt) signaling pathway, which leads to increased cell proliferation through rapamycin signaling (mTOR). EPAC proteins contain both a regulatory region (RR) and a catalytic region (CR) whose relative orientations with each other are determined by the conformation of an alpha-helix known as the hinge helix. The RR contains a cyclic nucleotide binding domain that binds cAMP and promotes a conformational change that opens the hinge helix and exposes the RAP binding pocket in the CR (Fig. 1). Once Rap proteins bind to EPAC, the CR facilitates exchange of GDP for GTP, which activates the GTPases and leads to downstream signaling changes.[18]

1.7 Role of EPAC in Cancer

EPAC is a prognostic marker for cancer and plays a role in its metastasis, because of its role in cell adhesion and cytoskeleton remodeling. Overexpression of EPAC allows for cancer cells to spread faster, allowing for the tumour to grow uncontrollably, this can be seen in human pancreatic ductal adenocarcinoma (PDA).[19]

1.7.1 ESI-09 prevents metastasis through EPAC inhibition

Small molecule inhibitors of EPAC have been designed to reduce cancer cells from spreading. The most well-characterized inhibitor is ESI-09 – a competitive allosteric inhibitor that displaces cAMP from the regulatory region.[20] In pancreatic cells, the drug blocks EPAC-mediated Rap1 activation, thus inhibiting pathway functions such as cell migration and invasion.

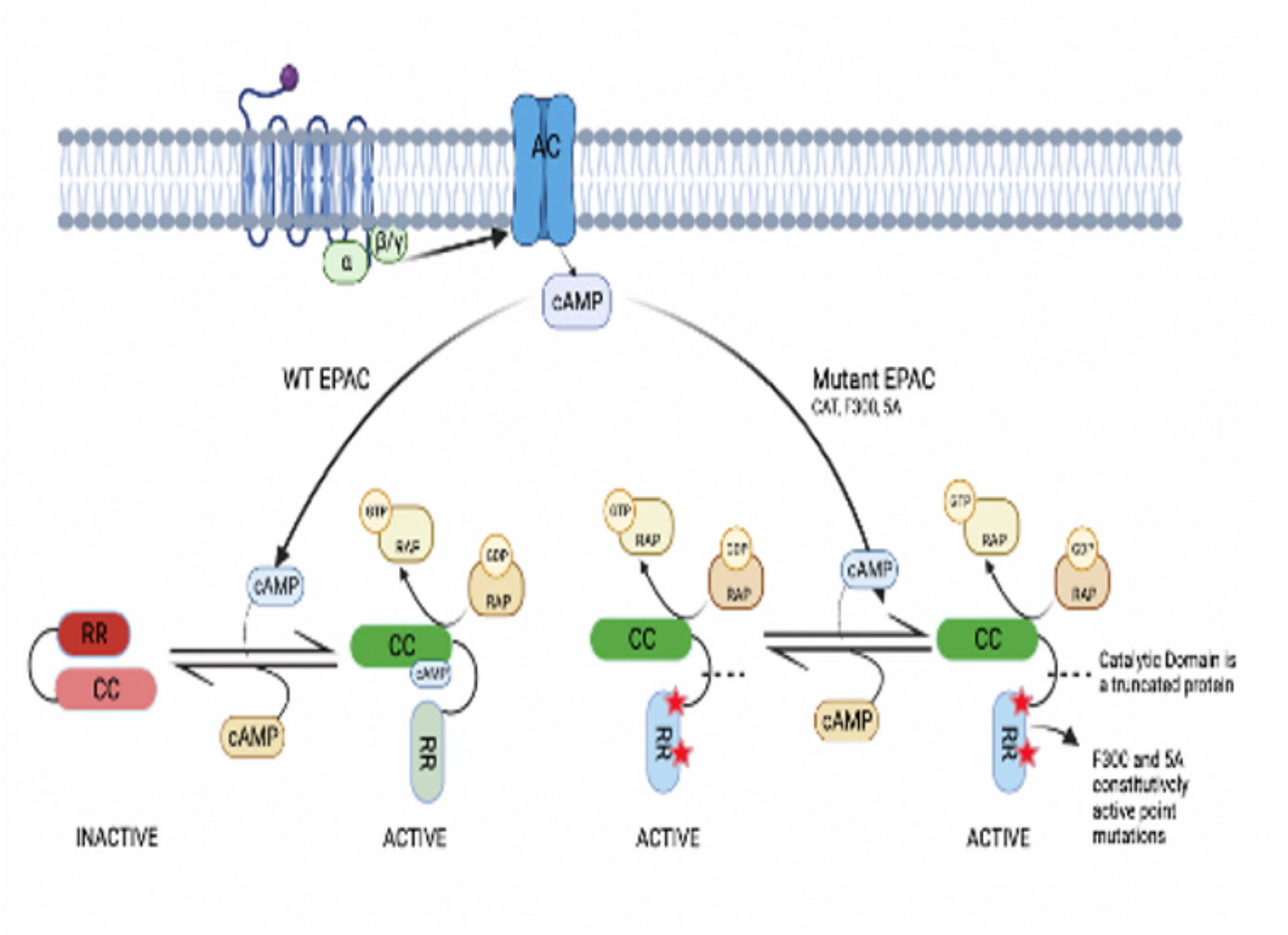

Figure 1: Schematic representation of the EPAC pathway in normal cells vs pathway when EPAC is render constitutively active via mutations in different regions of the protein (red stars)

Inhibiting EPAC using ESI-09 has also been shown to inhibit invasion and prevent micromets to the liver in murine pancreatic tumor models.[21]

While it would be potentially promising to incorporate the anti-metastatic properties of ESI-09 treatment with oncolytic and immune agonistic properties of OV therapy, we have found that ESI-09 acts as a potent broad-spectrum antiviral against a range of RNA and DNA viruses. In our group's own study, we found that EPAC inhibition via ESI-09 blocks multiple stages of the viral life cycle by remodeling the actin cytoskeleton.[22] ESI-09 induced remodeling of the cytoskeleton both prevents virus internalization via actin-controlled endocytosis pathways and inhibits cell-to-cell transmission of virus particles. The inhibitor is particularly effective at inhibiting virus-induced cell fusion (syncytia), which is an efficient strategy many viruses use to spread between cells without secreting virus particles that can be detected and neutralized by the immune system.[21]

1.8 EPAC activation synergizes with OV therapy

The role of EPAC in pathways that are important for virus infectivity and spread ensures that EPAC antagonism will interfere with the efficacy of OV therapies, but alternatively implies that EPAC agonism has the potential to enhance OV potency. Li et al. demonstrated that EPAC activation with the selective agonist 8-pCPT-2'-O-Me-cAMP-AM (007-AM) synergizes with oncolytic M1 alphavirus. This research was able to show a decrease in tumour burden in vitro and in-vivo in HCT-116, Hep3B and Capan-1 models. The paper concluded that EPAC specific activation enhanced M1 oncolytic effects in cancer cells while also inhibiting virus induce anti-viral factor expression, allowing for increased viral spread and decrease in tumor size.[23]

However, 007-AM is challenging to administer *in vivo* as a drug since it is sensitive to phosphodiesterase's in serum that eliminate its membrane permeability. This would likely mean the drug would be required to be administered directly into the tumour which would be challenging and limit is activity against metastatic tumours. 007-AM is also difficult to synthesize and expensive to purchase, so it is not easy to obtain high quantities that will be needed for *in vivo* administration.[24] Finally, while activating EPAC is beneficial for OV therapy, there can be many dangerous and harmful effects of activating off target EPAC in the patient's heart and lungs.[19] EPAC overexpression is already a prognostic for cancer and cancer metastases, thus off target activation will likely lead to disease progression. EPAC isoforms also have functions in insulin secretion which could be altered and finally could cause cardiac myopathies.[19]

1.9 Constitutively active EPAC expressed in an OV

The objective of this thesis was to encode EPAC into an OV, such as Vaccinia, so that it is expressed in only cancer cells and can help the virus to spread throughout the tumour. Since EPAC naturally exists in an auto-inhibited state, we also designed a series of mutations that would render EPAC constitutively active.[25] The constitutively active mutations used in this thesis are based on previous studies, which show induced activation in the absence of cAMP. They include the N-terminal RR deletion (CAT), the F300A point mutation and the VLVLE to AAAAA (5A) Lid mutations.[25,26]

As noted above, EPAC is divided into a regulatory region (RR) and catalytic region (CR). In the absence of cAMP the RAP binding pocket is occluded by the RR and when cAMP binds, the hinge helix that connects the two regions undergoes a conformational change that reorients the RR with respect to the CR and exposes the RAP binding site (Fig. 2A). The CAT construct simply

deleted the RR from EPAC and therefore prevents any occlusion of the Rap1 binding pocket. The N-terminal RR, however, also contains some domains that are important for cellular localization, so to ensure we can achieve constitutive EPAC activation without loss of localization, which might be essential for function, we also developed the F300A and 5A point mutations, which leave the N-terminal domains in tact.

The F300A mutation impact the hinge helix that controls the relative orientations of the RR and CR. In the native protein, the hinge helix conformation is controlled by a hydrophobic hinge composed of residues L273 and F300. [25] Due to steric clashes between F300 in the active hinge helix and L273 in the inactive conformation, the hinge cannot unfold until after cAMP binding and reorientation of L273. With the F300A mutation, the steric clash is removed between the two residues so since hinge helix is free to sample both active and inactive conformations without restraint (Fig. 2B).

For the 5A mutation, the VLVLE motif is part of a β-hairpin that connects the RR to the CR. Residue E325 of the motif also interacts with T210 in the RR when the protein is in its inactive "closed" topology (Fig. 2C). The VLVLE to AAAAA mutation breaks this interaction and destabilizes the β-hairpin structure resulting in shift to the active "open" topology.

As mentioned previously EPAC is a diagnostic marker for cancer and can actually aid in the progression of cancer.[19] Expressing the EPAC gene in the virus would allow for treatments that target EPAC in the body to continue to work without shutting down the viral EPAC transgene we design.

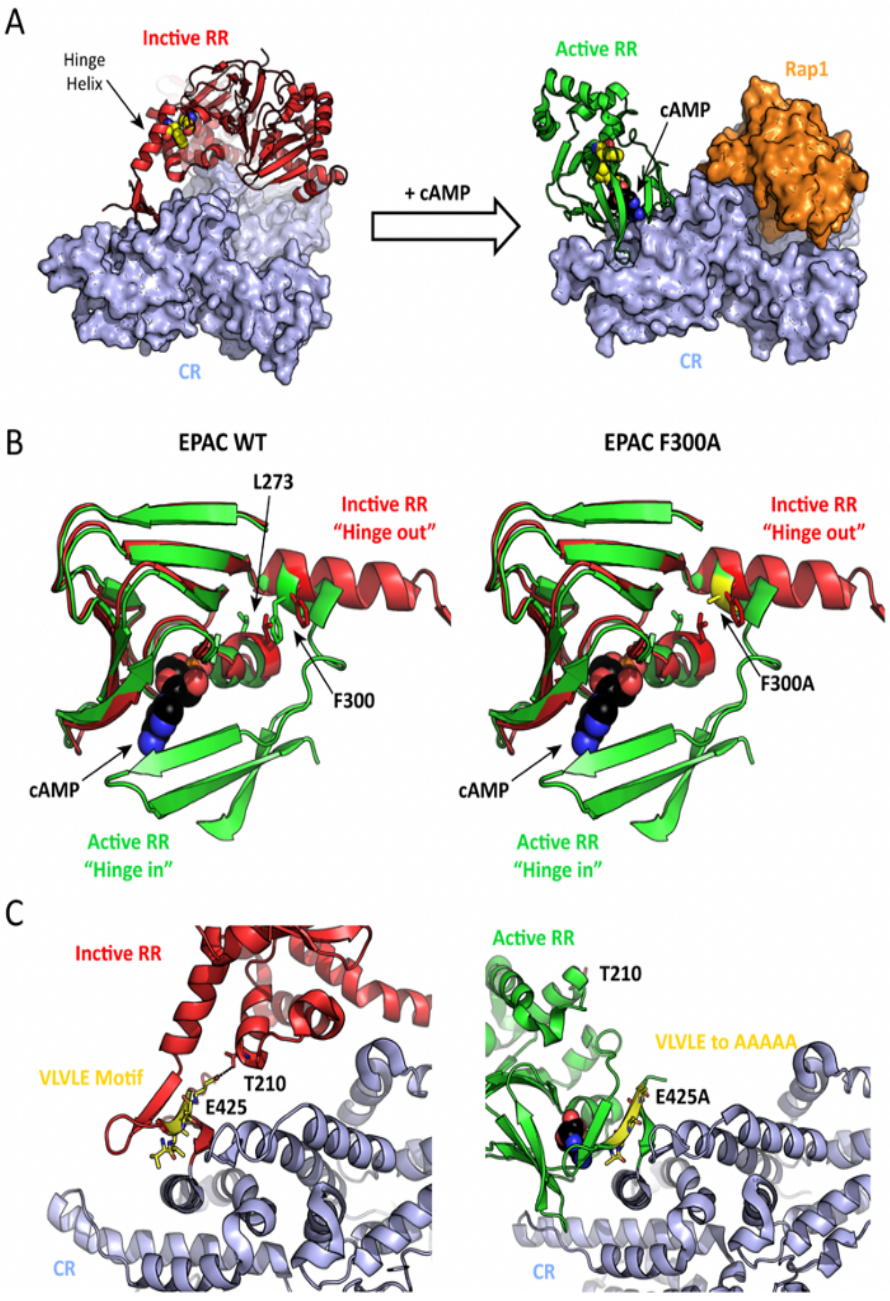

Figure 2: *EPAC conformational Equilibrium and Constitutive Activation Mutations.* **A)** Conformational changes in EPAC structure that occur in response to cAMP binding. The hinge helix in the inactive regulatory region (RR) partially unfolds and rotates the RR away from the catalytic region (CR) exposing the Rap binding pocket. **B)** Mechanism of the F300A mutation. **C)** Mechanism of the VLVLE to AAAAA (5A) mutation.

1.10 Combinational Drug Therapy

Since cancer is a disease driven by epigenetic reprograming and mutations, tumours often express many different subpopulations of cells.[3] These cells express distinct phenotypes and genotypes that behave differently which allows for a fluctuating tumour environment.

The development of constitutively active EPAC constructs expressed from oncolytic viruses can also pave the way for combinational therapy with the EPAC inhibitor ESI-09. Since the EPAC constructs are constitutively active, they will provide a resistance mechanism to the antiviral activity of ESI-09 and allow the virus to continually spread in its presence. However, ESI-09 will still main its anti-metastatic properties against the uninfected cancer cells in the tumor.

2.0 Hypothesis

I hypothesize that a cDNA encoding a constitutively active version of the EPAC protein in oncolytic vaccinia virus genome will increase viral spread and enhance survival of immunocompetent mice bearing colorectal or melanoma tumors.

Aims:

1) Characterize the mechanism by which EPAC activation improves the spread/efficacy of oncolytic vaccinia virus.
2) Assess the efficacy of oncolytic vaccinia viruses encoding constitutively active EPAC compared to virus controls to treat immunocompetent mice bearing colorectal or melanoma tumors.
3) Test the combination of EPAC expressing viruses with the anti-metastatic EPAC inhibitor ESI-09 and a potential synergistic therapy

3.0 *Materials and Methods*

3.1 Reagents, viruses, and cell lines

VACV Copenhagen strain was obtained from ATCC. Firefly luciferase and eGFP were inserted into VACV at the B14R locus under the control of an early/late promoter as described previously. VACV was cultured and tittered on U2OS cells using previously described methods. VSVΔ51 expressing eGFP 417 was used in this study.

All cell lines used in this study were acquired from American Type Culture Collection (ATCC) Cell lines were cultured either in DMEM or RPMI 453 supplemented with 10% fetal bovine serum (FBS).

3.2 Construction of Plasmids

The cDNA sequence of mouse EPAC1 (RAPGEF3) was derived from its mRNA sequence (https://www.uniprot.org/uniprotkb/Q8VCC8/entry). The sequence was codon optimized in SnapGene using *Mus musculus* codon tables. The EPAC CAT, F300A and 5A constructs were similarly designed in SnapGene. EPAC CAT spans residues 324-876 and is lacking the N-Terminal Disheveled, Egl-10, and Pleckstrin domain (DEP) was well as the cAMP-binding domain (CBD). The EPAC 5A constructs has the 5 residues 321-VLVLE-325 all mutated to alanine. The EPAC constructs also contain an N-terminal hexa-his tag and 3x FLAG tag followed by a GSG linker prior to the first residue of the EPAC sequence. The WT EPAC1 sequence was synthesized and cloned into pcDNA3.1 by Genscript. The remaining constructs were also cloned by Genscript using either site-directed mutagenesis or EZ cloning.

3.3 Fluorescence Microscopy

Viral infection of cells and cell morphology was assessed with direct detection of GFP under an EVOS M5000 microscope after the indicated time (24-48 hours).

3.4 Phalloidin Actin staining

U2OS cells were seeded onto glass coverslips in 6-well plates. Once cells had adhered, they were treated VACV and VACV EPAC mutants at an MOI of 3. Cells were then incubated for around 2 hours at 37 °C to allow virus attachment and entry. Cells were then fixed with 4% paraformaldehyde and in some instances permeabilized with 0.2% triton X-100. Cells were then blocked with 1% BSA for 30 minutes before staining with a polyclonal Vaccinia virus (1:1000; LS-C103289; LSBio) VACV infected cells were then washed and stained with an Alexa Flour anti-rabbit IgG secondary (A11037, Invitrogen), Coverslips were then mounted using prolong with DAPI (comp) and imaged with a Zeiss Axioskop 2 Epi-Fluorescence Microscope.

3.5 RAP1 FRET assay

RAP1 activation was determine using a FRET biosensor developed previously. A pLenti vector containing Rap1 fused to mCerulean3 and the Rap1-binding domain (RBD) of RalGDS fused to YPet was purchased from Addgene and used to generate stable cell lines in HEK293T cells. To probe for Rap1 activation, The HEK293T-Rap1-Biosensor cells were infected for 24 hours at an MOI of 0.05. They were then detached from their culture plates, resuspended in PBS and in a 96-well plate with 500,000 cells per well. Fluorescence was then measured using an excitation wavelength of 435 nm and emission wavelength of either 475 nm or 525 nm. The FRET

ratio was then computed by dividing the 525 nm emission by the 475 nm. For ESI-09 and 007-AM treatments, the compounds were added 60 minutes before reading.

3.6 Cell viability assays

Cells were incubated for 24 hours at 37°C with drug or virus of interest and viability was measured by an alamarblue cell viability assay (Life Technologies, Carlsbad, CA).

3.7 Plaque Assays

VACV titers were measured via standard plaque assay. Serial dilutions of each virus were prepared in SFM and infected into confluent 12-well plates U2OS (VACV) cells. Cells were incubated at 37 °C for 2 hours to allow virus attachment, following which the inoculum was removed and replaced with 1.5 % carboxymethyl cellulose (CMC) overlay. Cells were then incubated for 48 hours at 37 °C and then stained with crystal violet.

3.8 Antibodies and western blot analyses

Samples were collected by washing desired cells in PBS (1X) followed by washing in 500 ul RIPA Cell Lysis Buffer.) (RIPA Lysis Buffer: 25mM Tris-HCl pH7.5, 150mM NaCl, 1% NP-40, 1mM EDTA pH8.0. Added fresh: 1 mM PMSF, 1 mM Na3VO4, and 1 X Protease Inhibitor Cocktail-P2714, Sigma). After 20-minute incubation period on ice cell lysate was scraped and collected into Eppendorf tubes. The lysate was centrifuged in pre cooled centrifuge for 20 minutes and supernatant was collected and stored in -20 freezer.

15 ug of the lysate mentioned above was added to SDS Sample Buffer to make a final volume of 20 ul. Samples were boiled at 95 for 3 minutes and added to a pre-stained Bio-Rad SDS

page gel. The samples were run for 50-70 minutes until dye reached the bottom of the cassette. Gel was removed and soaked in transfer buffer (made by mixing Tris base 48.5 g, Glycine 240.2 g, Methanol 3.2 L, 10N NaOH 1.5 ml, add water to 16 L). Nitrocellulose was cut to the same size as the gel. Gel was transferred in tris-glycine buffer for 1 hour at 100V.

Membrane was washed with TBST (10mM Tris-HCl, pH 8.0, 150 mM NaCl, 0.05% Tween 20) 3 times for 5 minutes on shaker. Membrane was blocked with 5% skim milk for. 1 hour, and then washed 3 times for 5 minutes with TBST. Membrane was then incubated with FLAG (F1804-200UG) primary antibody overnight at 4c. Secondary mouse antibody (MAB402-SP) was added after washing for 30 minutes. Membrane was imaged using BIORAD Chemidoc imaging system.

3.9 Transwell Migration assay

BXPC3 cells 4e5 were seeded in a 12 well for 48 hours in 500ul of RPMI media. Day 2 the top chambers of 1-micron were coated with Matrigel (100ug/ml) and left to incubate for 1 hour at 37°C. Cells were then seeded on top chamber at 5e5 and left to incubate for 20 hours. Day 3, top chamber was infected with various viruses at an MO1 of **5** and left to incubate for 48 hours. Top chamber was removed and media was aspirated and cells were washed with PBS. 1ml of 1.5% crystal violet was added to bottom chamber and left to stain for 20 minutes.

3.10 Spheroid Model

BXPC3 cells were seeded at 2e4 in a round bottom 24 well plate with ____ media. After 48 hours viruses were added to the wells in SFM at an MOI of 1. Images were acquired after 24-48 hours after viral infection was visible under the microscopy machine.

3.11 Drug Inhibition Assay

U2OS cells were seeded at 1e6 overnight in a 6 well plate. Cells were then infected with the virus of interest in SFM at an MOI of 0.5 overnight. 24 hours post infection, 30ng/ml of Vaccinia inhibitor, Tecovirimat (Selleck Chemicals S3380) was added and left overnight. 48 hours post viral infection, images were acquired using M5000 EVOS microscope.

3.12 Wound-Healing Assay

U2OS cells were seeded at 1e6 overnight in 6 well. Cells were treated with ESI-09, 007-*AM* or DMSO. Pipette was scrapped along well to create a division in the cells. Images were taken immediately and after 48 hours.

3.13 Animal models

Mice were obtained from Charles River Laboratories (Wilmington, MA, USA). B16, MC38 tumours were established on the right flank. VACV was administered in 3 doses every other day after tumour reached ~ 4x4 mm via intratumoral injection.. Intraperitoneal models were injected on day 1 with MC38 cells and monitored daily until mice exhibited any symptoms and were end-pointed accordingly. Mice for metastases model were injected with B16 cells on day 1 and treated with drug on day 7. Drug injections were administered every day for 5 days. When the first tumor in the experiment reached 15x15mm, all mice were sacrificed and lungs were extracted to count mets. Experiments were preformed to protocol guidelines of the University of Ottawa animal care facilities.

3.14 Animal Imaging

Mice were injected with D-Luciferin for imaging. Mice were anesthetized under 3% isoflurane and imaged using the ACVS IVIS200 Series Imaging System.

4.0 Results

4.1 EPAC Agonism with 007-AM Enhances the Spread and Infiltration of Oncolytic Vaccinia Virus

As noted above, 007-AM improves the oncolytic activity of the ssRNA M1 alphavirus.[23]. Prior studies, which include our own work, have shown that EPAC antagonism inhibits replication of a variety of DNA and RNA as well as enveloped and non-enveloped viruses.[22] Hence, our first objective was to determine if there was a particular class of virus that synergized more effectively with EPAC agonism. I used a GFP reporter assay to measure the replication of four different OVs in cells that were treated with 007-AM and found that Vaccinia virus (VACV) was the only virus to significantly benefit from the 007-AM treatment (Fig. 3A). Therefore, we decided further test whether 007-AM could improve oncolytic VACV activity.

Pancreatic cancer model, BxPC3, has been the target of EPAC-related cancer studies in the past. Using this model, I determined if VACV-induced cytotoxicity could be increased with 007-AM (Fig. 3B).[24] For contrast, we showed that EPAC inhibition with ESI-09 led to a significant reduction in VACV-mediated killing, while EPAC activation with 007-AM led to a small but significant increase. Next, I examined how EPAC modulation would influence virus spread through a complex tumor-like environment. I developed a transwell migration assay where the virus was forced to spread from the top chamber, where BxPC3 cells were coated on a layer of Matrigel intended to simulate the extracellular matrix, to a bottom chamber of uninfected cells (Fig. 3C). A basal level of virus was able to migrate under mock conditions and infect the bottom layer of cells resulting in the formation of ~30 plaques. When cells were treated with ESI-09, the migration was halted and there was no observable spread of virus to the bottom chamber of cells. In contrast, cells treated with 007-AM led to a marked increase in the size and number of plaques in the bottom chamber of the transwell plate.

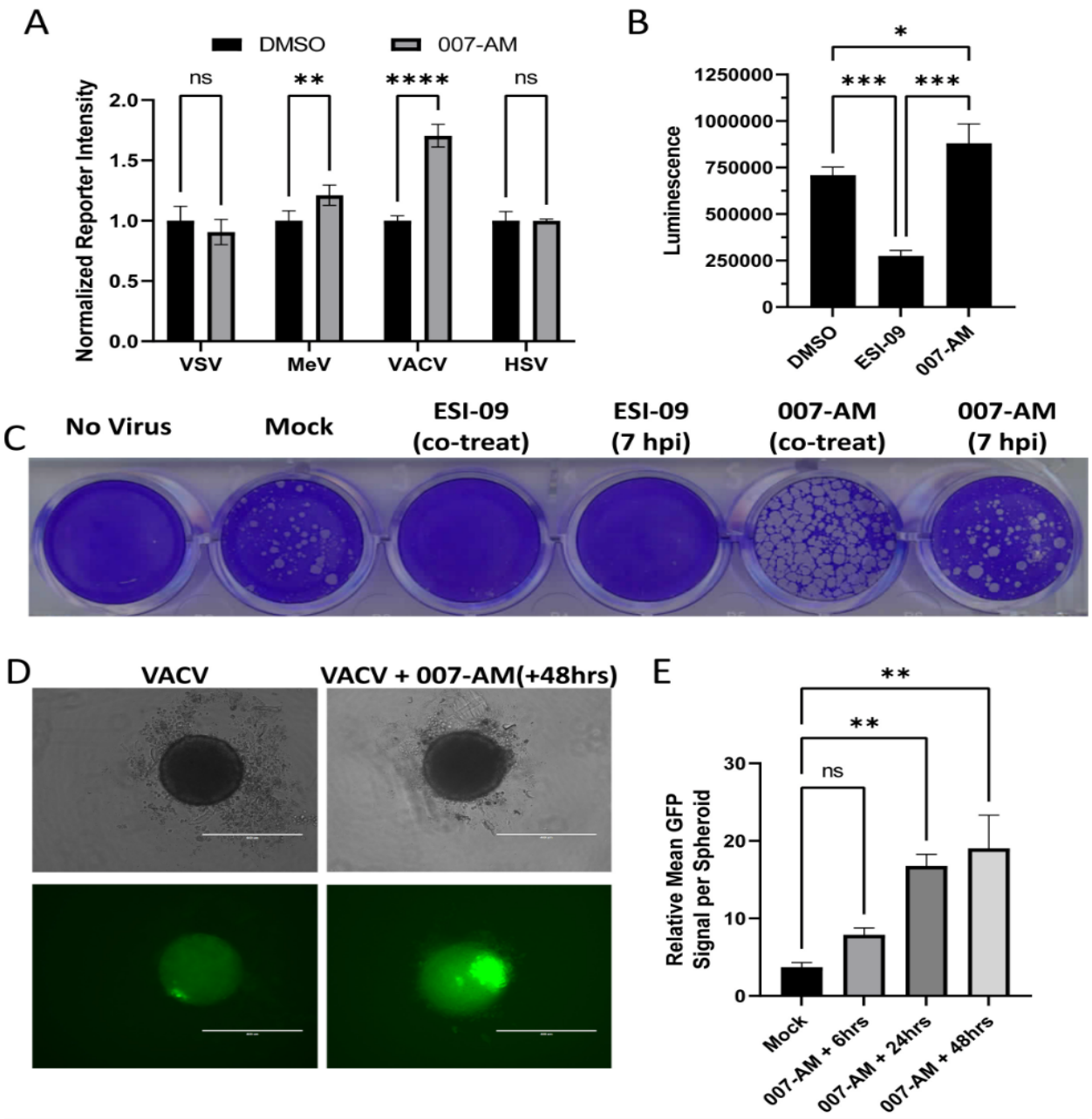

Figure 3: *EPAC agonism with 007-AM synergizes with oncolytic vaccinia virus infection.* **A)** Reporter growth assay for VSV, MeV, VACV and HSV in 007-AM treated cells. Cells were treated starting 2 hours before infection with 25 µM 007-AM and then infected with each of the indicated viruses at an MOI of 0.1. After 24-48 hours, virus infection was quantified by counting GFP expressing cells and normalizing to DMSO control. B**)** Nanoluciferase release assay in BxPC3 cells infected with VACV (at MOI 0.5) in the presence of ESI-09 or 007-AM. Supernatant was taken from cells 24 hours after infection. **C)** Virus Transwell migration assay. 0.1 µm Transwell inserts were coated with matrigel and a layer of BxPC3 cells then infected with VACV at an MOI of **1**. After 48 hours, the bottom chamber of the plate was stained with crystal violet to show plaque development. **D)** BxPC3 spheroids 72 hours after infection with VACV at an MOI of 0.1. 007-AM was added ,6, 24 and. 48 hours after infection. **E)** The mean GFP intensity per spheroid (n=3). Statistical significance was determined with ANOVA Fisher's LSD test (ns – 0.1234, * - 0.0332, ** - 0.0021, *** 0.0002, **** - 0.0001).

Lastly, to assess the synergy of 007-AM and VACV in a 3D-model I infected BxPC3 spheroids with virus at an MOI of 1. It can be seen the virus infiltrated farther in the spheroid model with 007-AM then untreated cells (Fig 3D). I also measure the mean GFP intensities in spheroids infected with VACV and treated with 007-AM at different stages after the infection (Fig. 3E). Doing so, I found that treating cells 24-48 hours after infection led to significantly higher levels of GFP expression compared to early treatment.

4.2 *Generation and Validation of EPAC-Expressing Vaccinia Virus*

After finding evidence that EPAC agonism improved oncolytic VACV replication and spread, we encoded either WT EPAC or its constitutively active mutants into the genome of the SKV strain of VACV. To confirm the expression of the various EPAC constructs in our SKV virus backbone we performed immunoblotting on lysates of infected cells with a FLAG antibody (Fig. 4A). I detected signal for all constructs at their expected molecular weights. To confirm that the EPAC constructs were catalytically active, we performed a Fluorescence Resonance Energy Transfer (FRET) assay, to look at activation of EPACs downstream target Rap1. The assay works by measuring FRET transfer between Rap1 and its downstream effector RalGDS, which only occurs when Rap1 is bound to GTP. To confirm the assay was sensitive to EPAC modulation, I measured Rap1 activation in our 293T-Rap biosensor cell line after treatment with DMSO, ESI-09 or 007-AM. It was seen when inhibitor (ESI-09) was added, activation decreased and when 007-AM was added, activation increased. All the viruses exhibited increased fluorescence compared to mock (Fig. 4B). WT SKV was low relative to the EPAC mutant viruses. The CAT mutant had the highest ratio. I also confirmed that GFP expressed from the virus did not interfere with the biosensor FRET resonance which used CFP and YFP proteins that have similar emission and excitation wavelengths (Fig. 5).

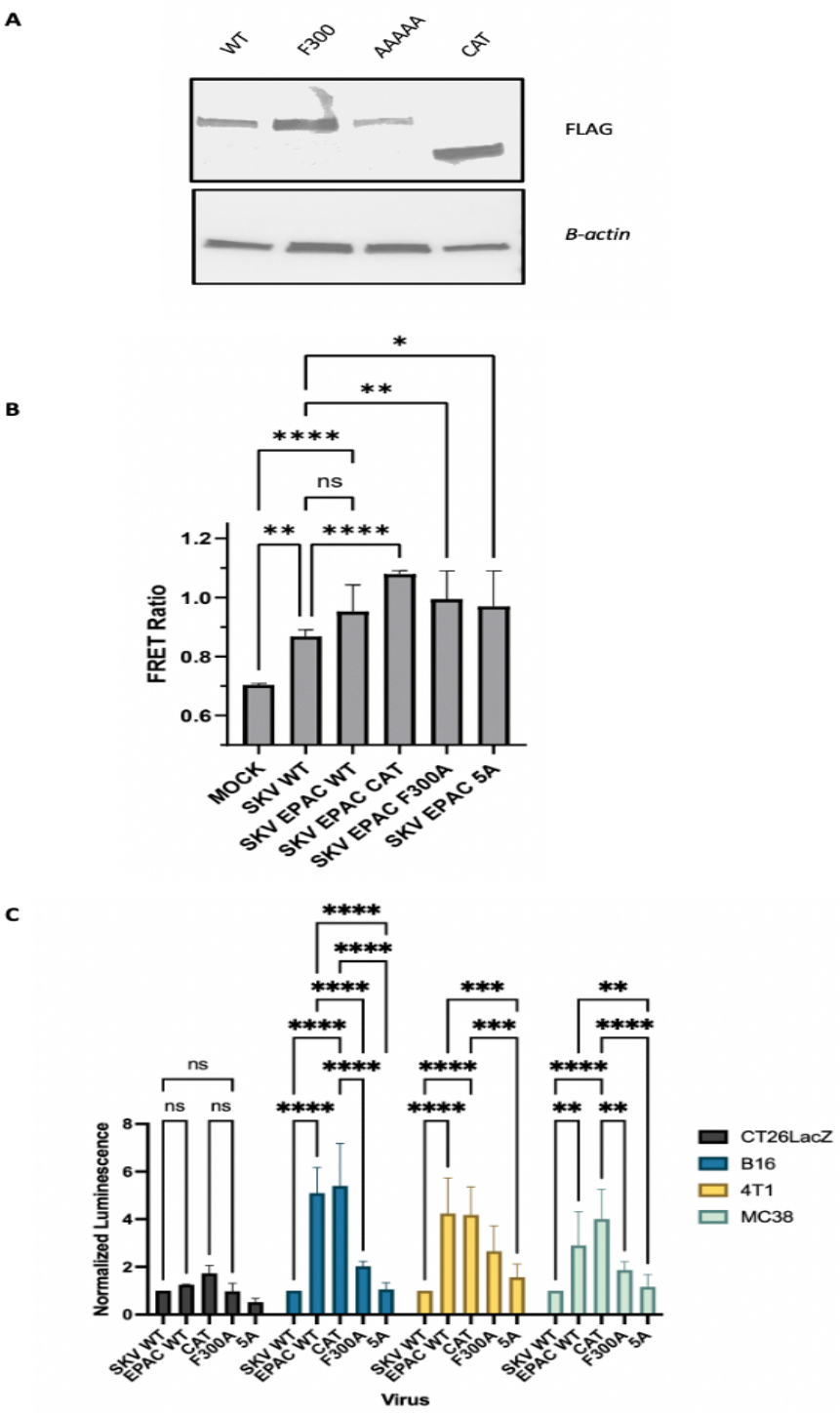

Figure 4. Validation of EPAC expression (A) Model of EPAC pathway in normal cells vs pathway when EPAC is render constitutively active via mutations in different regions of the protein (red stars). (B) Immunoblot confirming expression of the various EPAC mutations in each SKV virus. B-actin loading control also shown. (C) FRET ratio confirming activity status of EPAC. (D) Luminescence readout of a range of mouse cancer cell lines infected with mutant EPAC viruses. Statistical significance was determined with ANOVA Fisher's LSD test (ns – 0.1234, * - 0.0332, ** - 0.0021, *** 0.0002, **** - 0.0001).

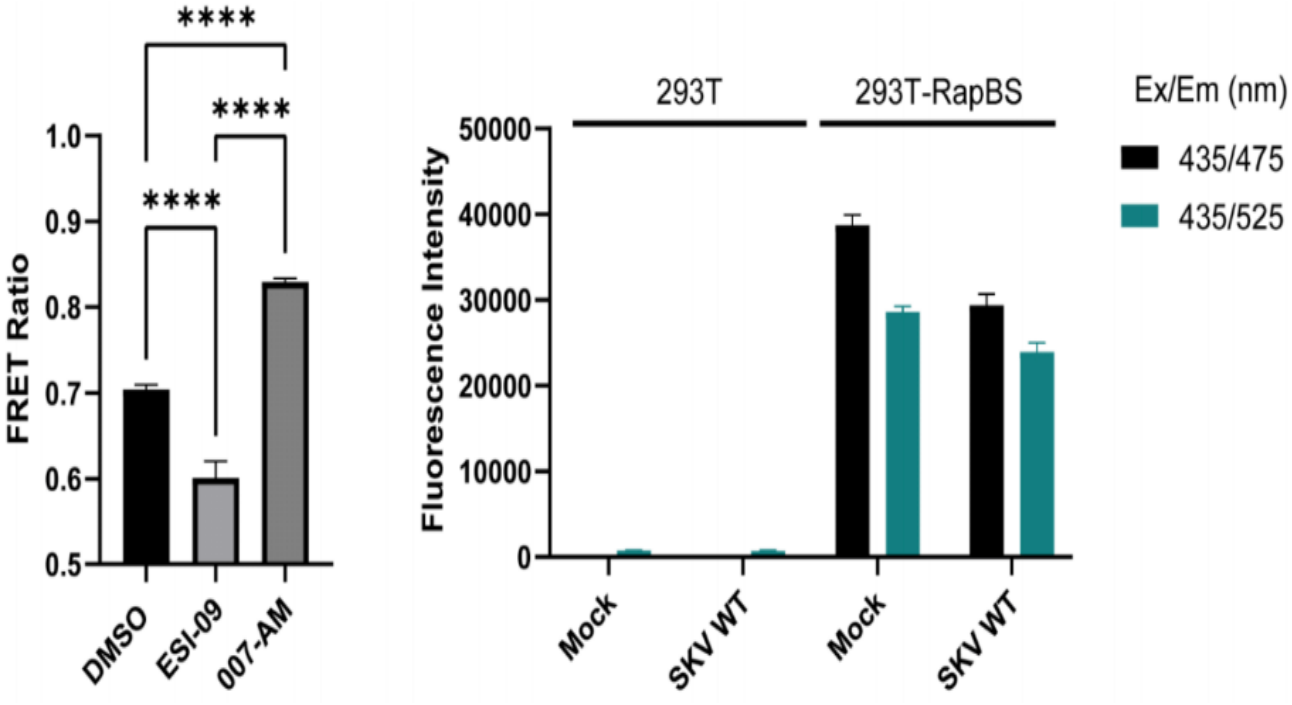

Figure 5. FRET controls Statistical significance was determined with ANOVA Fisher's LSD test (ns – 0.1234, * - 0.0332, ** - 0.0021, *** 0.0002, **** - 0.0001).

After confirming the activity of the mutant viruses, a panel of commonly used mouse cells lines: B16, MC38, 4T1 and CT26LacZ were infected to determine which cell lines were more susceptible to viral spread via overactive EPAC (Fig. 4C). It was observed using luminescence that viral infection was much higher in B16 cells and MC38 cells infected with mutant virus, relative to WT SKV infected cell lines. Our mutant CAT virus had the highest infection in both B16 and MC38 cells and was comparable to WT EPAC in 4T1 cells. In all cases our mutant CAT and F300A EPAC viruses were more effective at infecting the cell line than was WT SKV.

4.3 Mutant EPAC viruses alter plaque morphology

EPAC viruses led to a change in plaque morphology marked by an increase in cell fusion. (Fig. 6A) This consequently led to larger plaque formation. This agrees with our previous data that showed that EPAC inhibition could block syncytia formation. EPAC mutant infected cells had over a 50% increase in diameter compared to WT SKV. CAT mutant had the largest plaques at both 24-hour and 48-hour time points. (Fig. 6B)

4.4 EPAC plays a significant role in actin remodeling

Previous work done by Boulton et al., showed that EPAC inhibition via ESI-09 led to extensive actin cytoskeleton remodelling so I sought out to investigate the effect on actin formation with our overactive EPAC viruses. After staining cellular actin with a fluorescent phalloidin dye, we similarly found extensive changes to the actin cytoskeleton between uninfected, WT VACV infected and VACV-EPAC infected cells (Fig. 6C). In uninfected cells, there was a high degree of linearized stress fibers localized throughout the cytosol. These stress fibers were notably absent or significantly reduced in all of the infected samples. In the VACV-EPAC infected

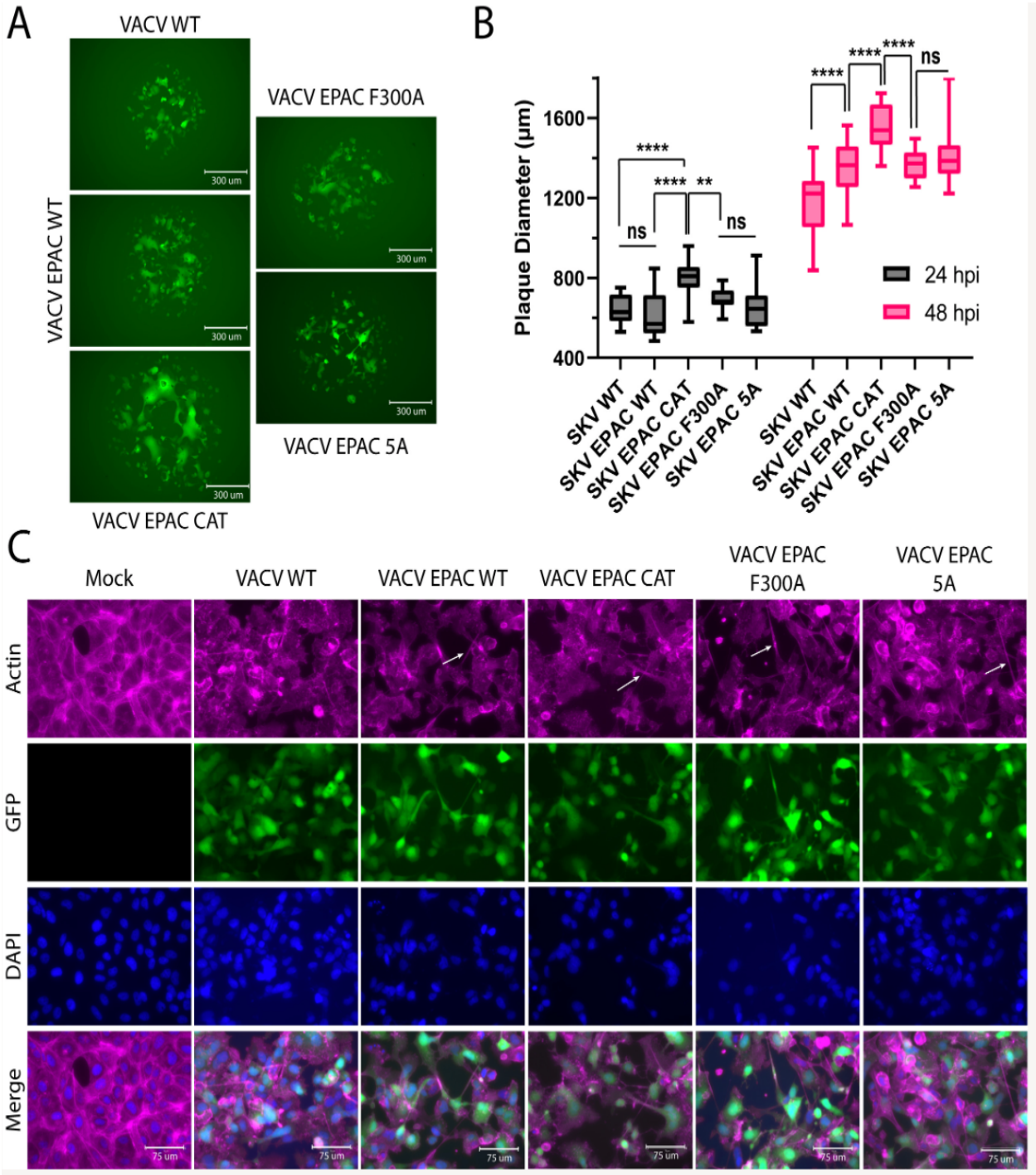

Figure 6. (A) Comparison of plaque formation by different mutant EPAC SKV viruses in U2OS cells. (B) Average plaque diameter of mutant EPAC viruses at 24 hpi (grey) and 48 hpi (pink). (C) Phalloidin staining of actin filaments in Vero cells infected with different viruses. Statistical significance was determined with ANOVA Fisher's LSD test (ns – 0.1234, * - 0.0332, ** - 0.0021, *** 0.0002, **** - 0.0001).

cells, we observed the formation of nanotubes connecting cells over long distances. These nanotubes may serve as bridges to transmit virus particles directly between cells.

4.5 Tecovirimat has no effect on mutant EPAC mutant viruses

To confirm the findings that mutant EPAC viruses are more infectious because of syncytia, we infected U2OS cells with both our virus and Tecovirimat, a drug known to inhibit the spread of VACV. Tecovirimat works by inhibiting the P37 protein which interacts with downstream RAB9 GTPase and TlP47 which is essential for the formation of egress-competent enveloped virions.[30] It was seen 24 hours post infection that cell-to-cell viral transmission was greatly affected in cells not treated with mutant EPAC viruses. (Fig. 7A) Again, it can be seen that both CAT and F300A are not affected by the drug indicating that our EPAC mutants enhance syncytia allowing for increase viral infection.

Previous data showed 007-AM in combination with virus increased viral spread in transwell and spheroid models. I re-preformed the same experiments with our viruses to see if the EPAC mutants provided the same benefits.

4.6EPAC mutant viruses had increased infection throughout BxPC3 spheroids mimicking a tumour environment.

I hypothesized that because of the increased syncytia and actin remodelling in our EPAC mutants, we would see greater viral infection in a tumour simulated environment. I imaged the spheroids after 48 hours using the EVOS and observed that SKV WT and EPAC WT viruses were not able to penetrate the entire spheroid in 48 hours. When examining the CAT and F300A mutant viruses I saw that the infection had spread to the center of the spheroid demonstrating

that our viruses improve viral spread in a tumour environment. This indicated that the virus could spread from cell to cell faster than the wildtype SKV virus. (Fig. 7B)

I observed in the transwell/migration assay that both mutant EPAC viruses were able to penetrate through the Matrigel to the bottom chamber better than WT SKV. Notably, WT EPAC also had more plaques in the bottom chamber compared to WT SKV. This prompted me to conclude that mutant EPAC would be more infectious than WT SKV, in a tumour environment (Fig. 7C)

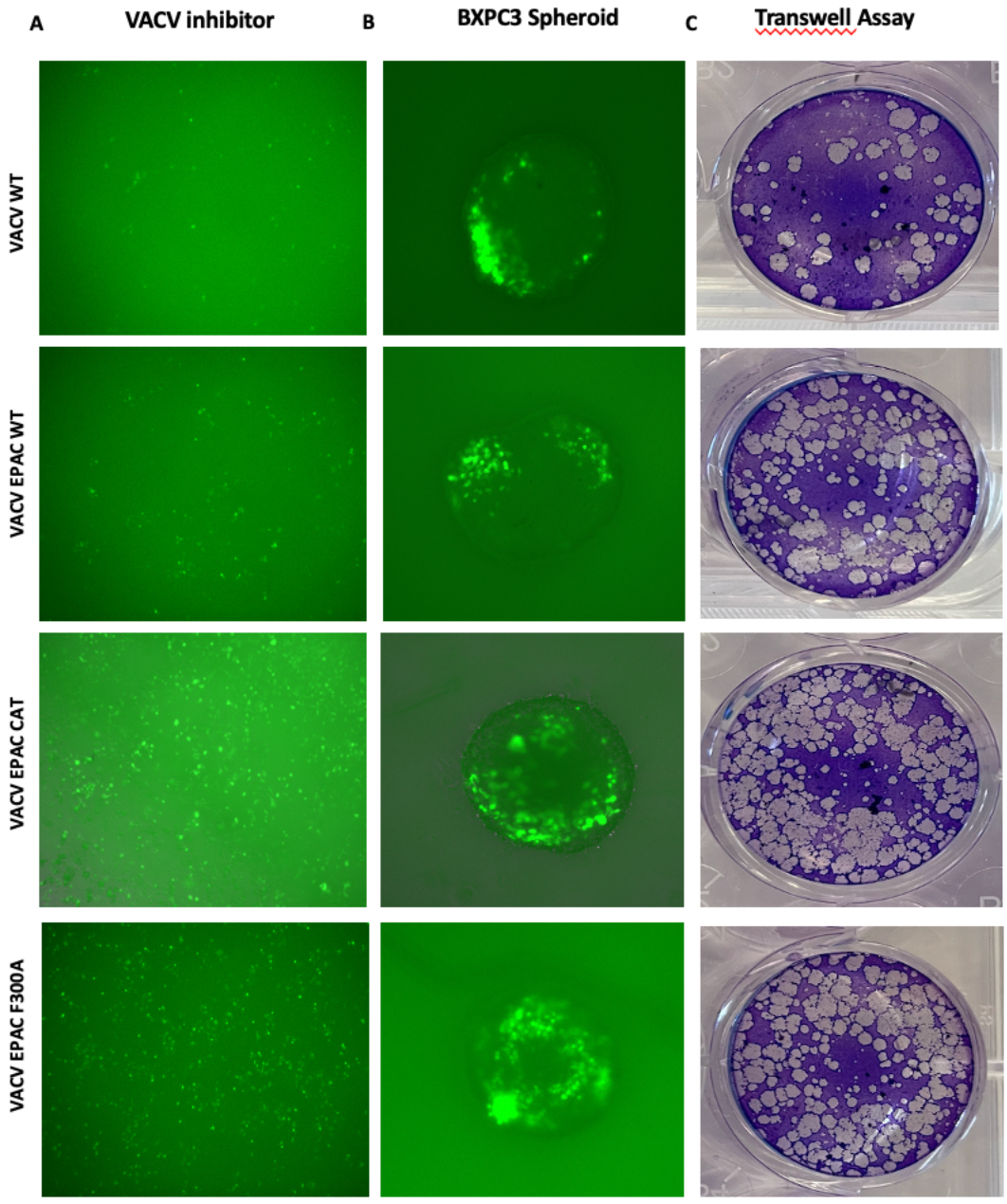

Figure 7. (A) The effects of tax a VACV virus inhibitor drug on cells infected with various EPAC viruses. (B) Spheroid BxPC3 cells infected with EPAC mutant viruses. (C) Virus Transwell migration assay. 0.1 µm Transwell inserts were coated with matrigel and a layer of BxPC3 cells then infected with VACV at an MOI of **1**. After 48 hours, the bottom chamber of the plate was stained with crystal violet to show plaque development.

4.7 Virus replicates in mouse model

To confirm viruses were replicating in-vivo models, mice were seeded with subcutaneous B16 tumors and grown to ~ 5x5mm and treated with SKV and each of the mutant EPAC groups. Viral replication was measured using IVIS 4 days after initial infection (Fig. 7A). Luciferase levels were consistent amongst all the groups (Fig. 7B) indicating replication in all the groups but were notably high in SKV group mouse 1, CAT group mouse 4 and F300A group mouse 2.(Fig. 7A) Following treatment mice were examined daily and were end-pointed when the mouse exhibited any symptoms outlined by the Ottawa Hospital Animal Care Facilities or when the tumor reached 15x15mm. While PBS injected mice succumbed first, we did not see a significant difference between our control virus and experimental viruses initially. We did however have 2 survivor mice, one in each of our experimental groups. These mice were CAT group mouse 4 and F300A group mouse 2, the two mice with the highest luciferase readout potentially indicating increased replication of our mutant. To confirm the mice were cured we rechallenged the two survivors and a placebo mouse, not previously treated with B16 cells and repeated the experiment. The two experimental mice recovered from SKV F300A and SKV CAT, and the placebo mouse was end pointed at ~ 15x15 on day 18. (Fig. 8D)

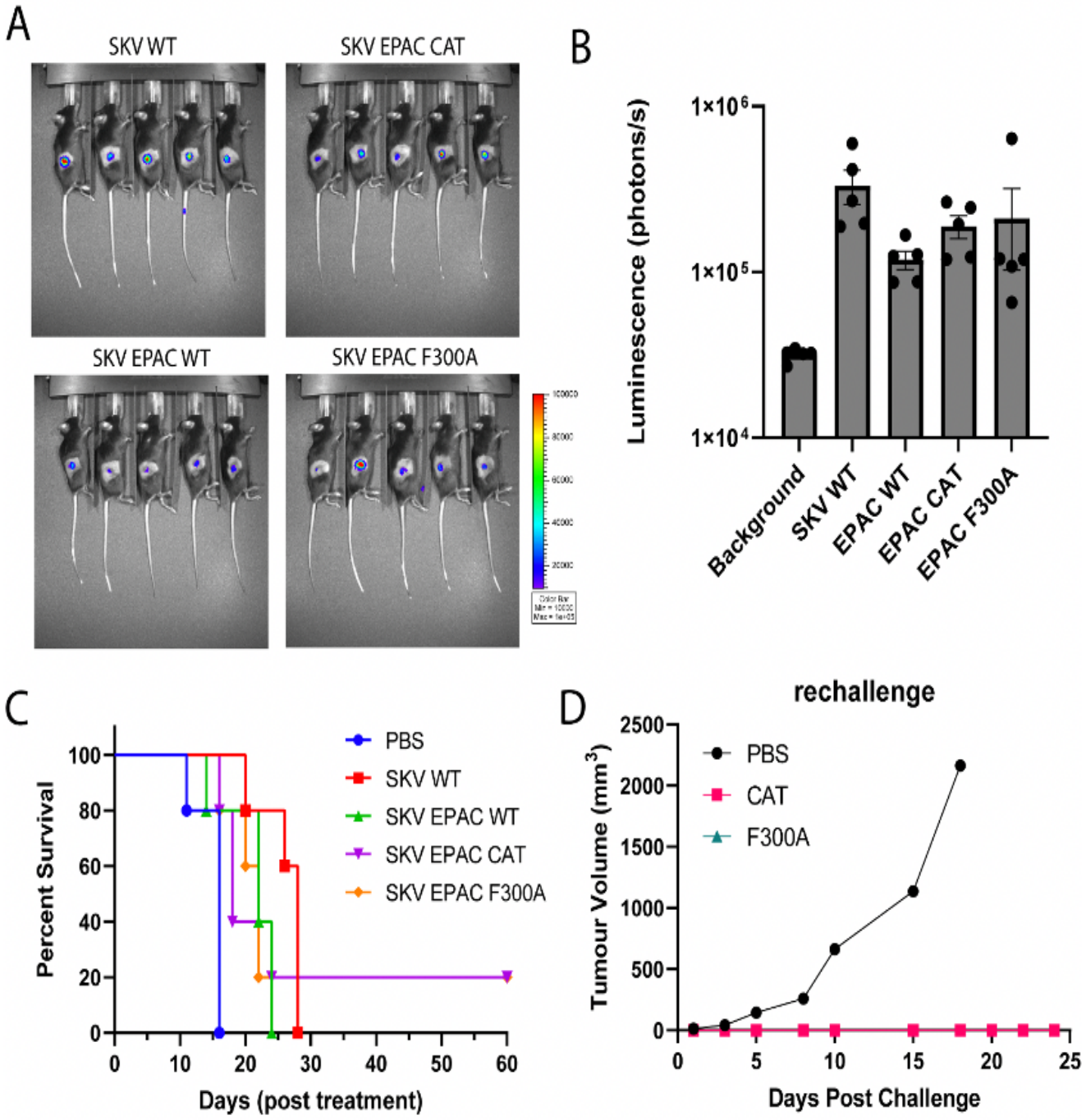

Figure 8. (A) IVIS imaging 4 days post infection. (B) Average luciferase readout per group. (C) Survival plots of each experimental in-vivo group, 60 days indicating survival. (D) Survival plots of rechallenged survivor mice from panel C, 25 days indicating survival. Statistical significance was determined with ANOVA Fisher's LSD test (ns – 0.1234, * - 0.0332, ** - 0.0021, *** 0.0002, **** - 0.0001).

Because mutant EPAC viruses had a high viral response in both B16 cells and MC38 cells in-vitro (Fig. 4D) I repeated the first in-vivo model but with MC38 sub-cutaneous tumors. I designed a 2nd set of viruses containing the same EPAC mutations but with the Tiantan (TT) VACV strain containing the A56R gene deletion. TT is a less attenuated version of VACV that has better persistence when replicating in mouse tumors than SKV.[30] Hence we expect benefits from EPAC expression to be enhanced in the TT backbone. I added the A56R gene deletion, which encodes hemagglutinin, since it attenuates the backbone slightly and improves safety and selectivity for tumors, while also promoting a fusogenic phenotype, which we believe will synergize without EPAC constructs. I generated and tested the TTΔA56R mutant EPAC viruses in vitro and found they created larger plaques with an increasingly fusogenic phenotype. However, at this point I am still generating the TTΔA56R EPAC WT virus and trying to reproduce in vitro results, which we previously described for SKV. Going forward, I will attempt to compare TTΔA56R with SKV viruses head-to-head in vivo experiments.

Injections were given on day 1,3, and 5. Following injections mice were measured and observed in accordance with animal care guidelines and end pointed when tumours reached ~15x15. (Fig. 8A). TTΔA56R mutant EPAC viruses had smaller tumors sizes compared to SKV mutant EPAC viruses. Data was recorded until first mouse was end pointed in each group. Tumour sizes were smaller on average in the TTΔA56R experimental groups than the SKV experimental groups (Fig 9. A,B). F300A mutant was seen to have the greatest success within the SKV experiment but not by a significant amount. I observed a greater difference in the TTΔA56R

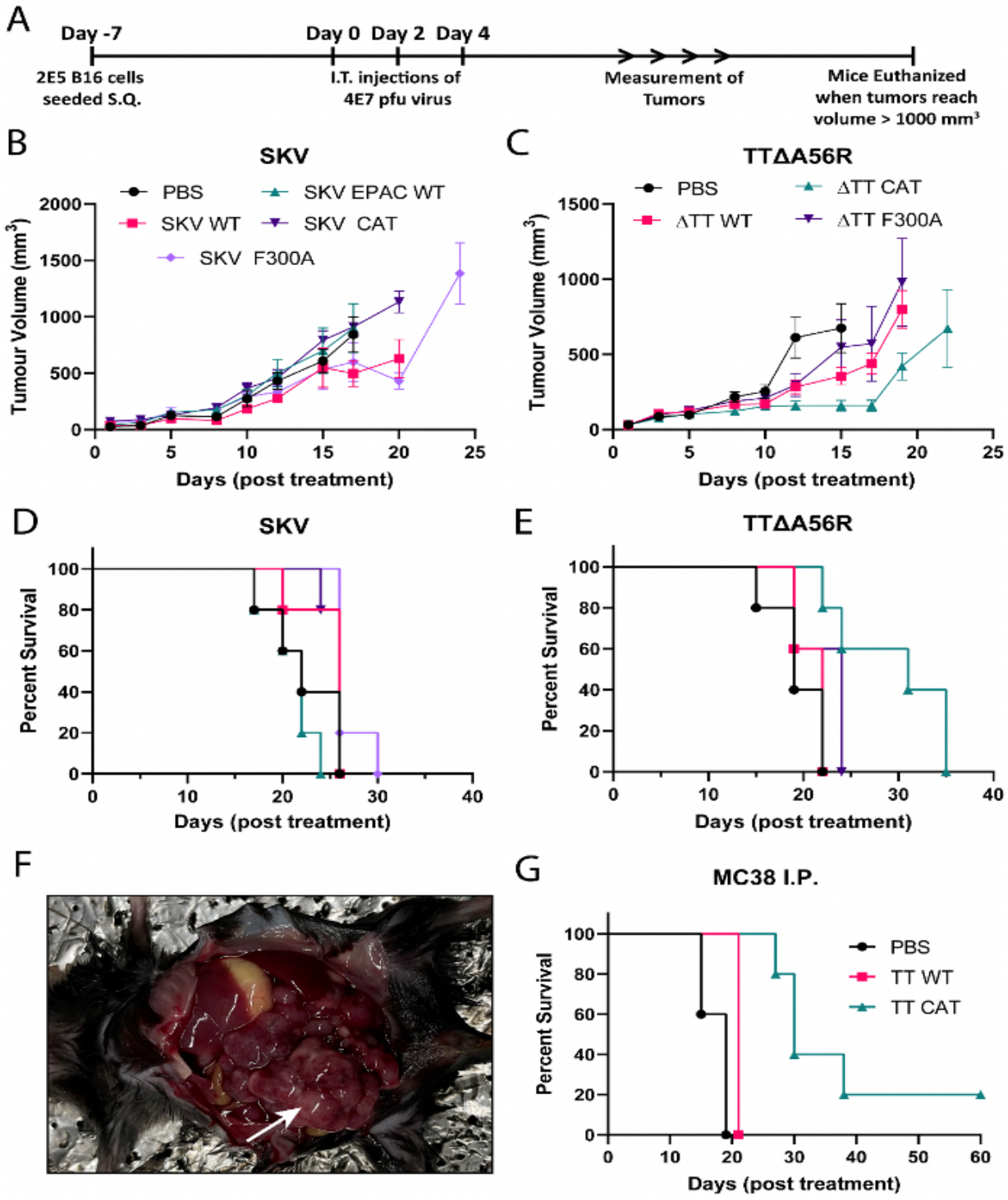

Figure 9. (A) Overview of in-vivo experiment timeline. (B) Volume (mm^3) of MC38 tumors treated with SKV mutant EPAC strains starting 7 dpi until first mouse in group was end-pointed.(C) . Volume (mm^3) of MC38 tumors treated with TTΔA56R mutant EPAC strains starting 7 dpi until first mouse in group was end-pointed.

(D) Survival plot for mice from panel B. (E) Survival plot for mice from panel C. (F) Image of intraperitoneal tumor. (G) Survival plot for mice with IP, TTΔA56R infected.

groups. Within the TTΔA56R virus groups we can see that the CAT mutant group had smaller tumour measurements consistently (Fig. 9C). There was an even greater difference between the two virus strains when studying the survival proportions. CAT mutant mice had a 50% survival rate past 30 days in TTΔA56R model (Fig. 9C) whereas all mice treated with SKV viruses were end pointed by day 30 (Fig. 9D). F300A mutant 50% survival was close in both TTΔA56R and SKV at 24 and 26 days respectively. Due to the success, we had with the TTΔA56R CAT mutant group, this is the group I chose to continue with in the rest of our in-vivos to limit costs associated with animal care facilities.

4.8 CAT mutant with TTΔA56R virus had higher survival proportions with IP model

With the previous TTΔA56R data showing promise, I examined how the virus would hold up against a more aggressive cancer model. I injected MC38 cells into the intra-peritoneal (I.P.) space on day 1 and injected with the TTΔA56R virus, and mutant TTΔA56R CAT virus I.P. on day 7. Since I could not measure the tumours internally, I followed the guidelines outlined by animal care and end pointed the mice when the exhibited more than 1 of the following symptoms: hunched posture, decrease in activity, extreme abdominal distention, skin lesions or tachypnea.[32] After endpoint, I confirmed tumor presence by autopsying the corpses (Fig. 9F). Our 50% survival for PBS, WT TTΔA56R, and TTΔA56R CAT were 15, 21 and 27 days respectively. All mice in the placebo (PBS) and control groups were end pointed by day 23 and mice in TTΔA56R CAT mutant group were end-pointed 15 days later on day 38 with one survivor represented by day 60. (Fig. 9G)

4.9 Wound healing assay shows ESI-09 blocks cell migration

With the promise of TTΔA56R CAT mutant decreasing tumour burden both *in-vitro* and *in-vivo* I began to investigate using ESI-09 as an anti-cancer drug in synergy with our mutant TTΔA56R EPAC viruses. As mentioned earlier ESI-09 inhibits EPAC, which plays a vital role in cell-cell adhesion. To confirm this, I performed a wound healing assay. It can be seen after 48 hours that cells treated with ESI-09 were not able to recover whereas cells treated with an EPAC activator (007-AM) were (Fig. 10A) This phenomenon can be seen again when conduction a transwell migration assay. Cells treated with ESI-09 had a significant decrease in cells able to migrate through the matrigel to the bottom chamber compared to DMSO treated cells. (Fig. 9B)

4.10 ESI-09 shows potential in preventing metastases to the lungs

The goal of designing a virus unaffected by EPAC inhibitors such as ESI-09 is, to have a virus will both decrease tumour burden and remain unaffected by drugs inhibiting host EPAC designed to decrease tumour metastases. While the literature confirms ES019 decreases tumor metastases to the lungs I attempted to create a model to confirm these findings.[21] Mice were injected with subcutaneous B16 tumours, and 7 days later were injected with 7 consecutive ESI-09 drug injections every day, both IP and IT. Mice were measured every 2 days until first tumor in any group reached 15x15mm (Fig 10F) . Mice lungs were extracted and metastases were counted. The mice that received ESI- 09 did not have metastases in the lungs. Mice that did not receive any

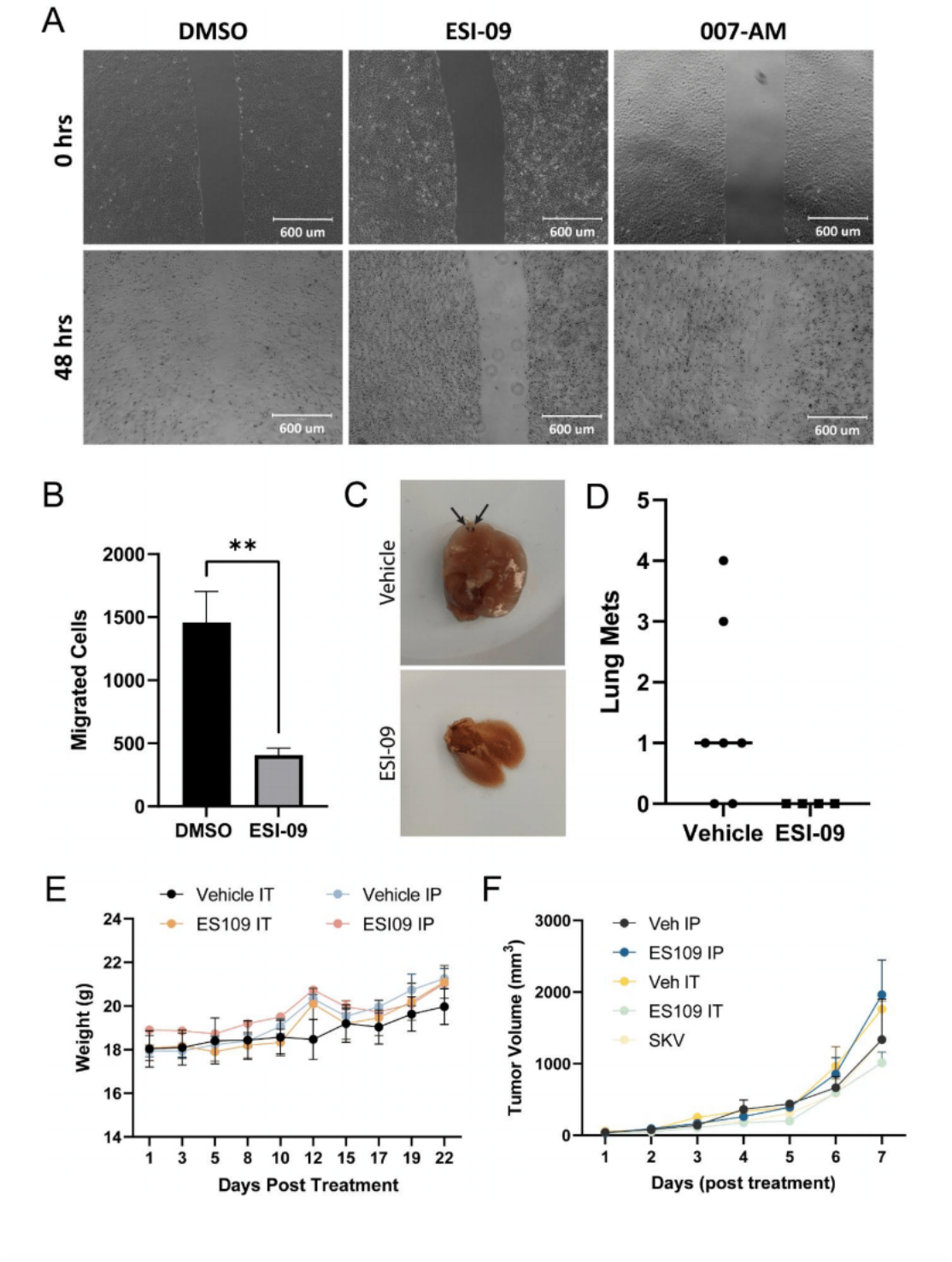

Figure 10. (A) U20S cells scrapped with pipette treated with drugs of DMSO. (B) Analysis of migrated cells from panel A. (C) Images of mouse lungs removed to show METS. (D) Analysis of the number of METS in lungs after treatment in vehicle and treatment groups. (D) Relative weight loss in mice receiving 250 μM ESI-09 or vehicle. (E) Volume (mm^3) of B16 tumors treated with ESIO9 starting 7 dpi until mice were sacrificed for lungs. Statistical significance was determined with ANOVA Fisher's LSD test (ns – 0.1234, * - 0.0332, ** - 0.0021, *** 0.0002, **** - 0.0001).

drug had at least one metastasis in the lung (Fig. 10C). Due to the low number of metastases observed, a more in depth model is required to validate the results of ESI-09. (10D) I was able to confirm through weights that the drug was not toxic to the mice as weights were not affected by the drug (Fig. 10E).

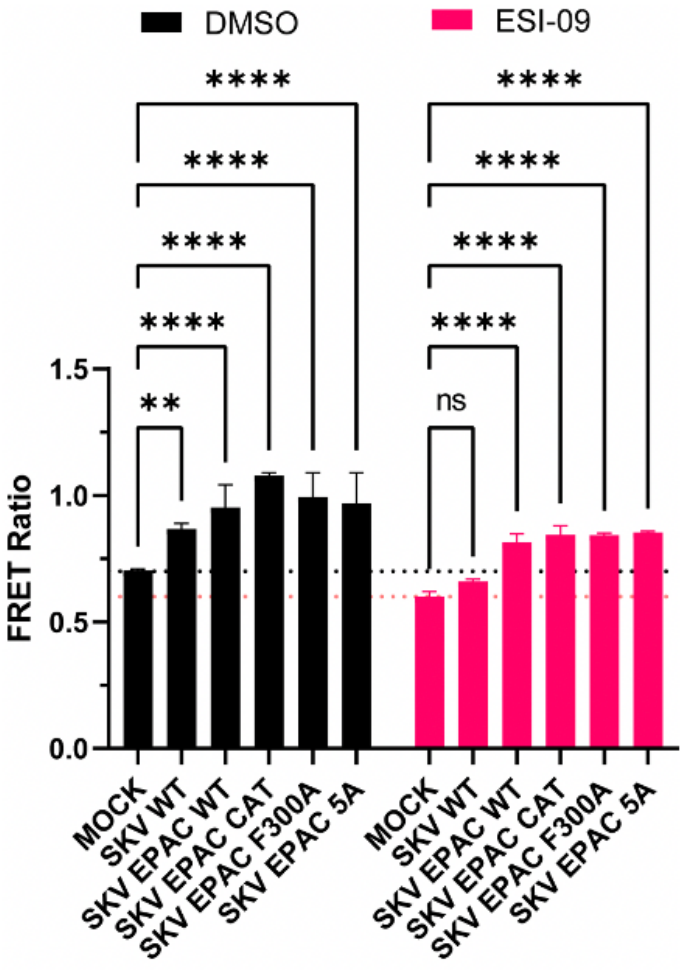

Figure 11. RAP1 stable cells infected with EPAC mutants viruses while receiving either DMSO or 25 μM ESI-09 drug treatment. Statistical significance was determined with ANOVA Fisher's LSD test (ns – 0.1234, * - 0.0332, ** - 0.0021, *** 0.0002, **** - 0.0001).

It was seen previously in the Rap1 stable cell line, cells treated with ESI-09 showed a decrease in activation. I wanted to see the effect ESI-09 would have on our mutant EPAC viruses.

A slight decrease in FRET efficiency can be observed in all our mutant viruses in the presence of ESI-09, but an even greater decrease in SKV WT. SKV WT was only slightly better than mock but not significant. (Fig. 11)

5.0 Discussion

Cancer immunotherapy is a relatively new treatment paradigm that holds great promise in the future for patients suffering from malignant tumours. OV's in particular are promising immunotherapies with the ability to deliver therapeutic payloads, promote tumor cell death and generate host antitumor immunity. In this thesis, we designed a novel transgene based on the catalytic region of EPAC1 and showed that EPAC activation in cancer cells drives OV replication and improves therapeutic efficacy *in vivo*.

The transgene we investigated in our study is EPAC, a signalling protein that regulates processes such as cell proliferation, cell adhesion, invasion and migration. We created constitutively active EPAC via point mutations 5A and F300A or deletion of the regulatory domain for CAT. Since EPAC is responsible for migration and invasion properties, we hypothesized that an OV that overexpressed active EPAC would be able to spread and replicate faster in a tumor environment and that this would increase OV-mediated tumor cell lysis.

VACV harboring constitutively active EPAC constructs were able to replicate and spread better compared to WT strains in both SKV and TTΔA56R backbones. Furthermore, we show that constitutively active EPAC can increase plaque size and promote cell-to-cell fusion (syncytia). These findings are consistent with our previous results (Boulton et al. under review) that show ESI-09 (an EPAC inhibitor) blocks viral replication by inhibiting cell-to-cell transmission and cell fusion. In our case, we show that activating EPAC has the opposite effect leading to enhanced syncytia and viral spread.

We also observed, similar to previous findings in our group's previous study (Boulton et al. under review), that EPAC modulation leads to extensive actin cytoskeleton remodeling. Here, we found that EPAC activation led to a reduction in stress fibers and an increase in

nanotube-like structures between cells, which we predict provides bridges for virus particles to spread directly between cells without being secreted. We confirmed this theory by adding Tecovirimat, an antiviral drug that inhibits VACV egress, to the cells infected with our VACV viruses. SKV WT replication was hindered by the drug significantly, while EPAC viruses were still able to replicate and spread, which indicates they were able to adopt another strategy to spread between cells without virion released.

Based on the evidence that EPAC improves virus cell-to-cell transmission, we expected that it would improve virus spread in complex 3D environments and we found with our transwell and spheroid experiments, the results supported this. In both transwell and spheroid models that CAT and F300A increased viral spread and promoted cancer cell death. In the spheroid model, the CAT and F300A viruses had more virus spread throughout the spheroid compared to SKV WT.

A variety of *in vivo* models were used to test the efficacy of EPAC-viruses in relieving tumour burden and improving survival. These include a B16 and MC38 S.Q. models as well as an MC38 IP model. We chose these models since they had the largest differences in SKV replication between WT and EPAC viruses *in vitro* (Fig. 4C). For the B16 S.Q. model we didn't observe significant changes in tumor sizes or rates of survival, but we had two survivors from groups treated with the EPAC viruses, while there were zero survivors from the SKV WT and PBS treated groups.

While SKV is a promising OV candidate, because of its selectivity and immunogenicity, which drive anti-tumor immune responses, it does suffer from being more attenuated. This reduces its persistence *in vivo*. Some transgene therapies work synergistically with the immunogenic phenotype of SKV, while others require prolonged expression or better virus

survival to have an effect. Therefore, we also encoded the EPAC constructs into an attenuated Tiantan (TT) strain of VACV that we designed and used previously as a vaccine vector (Boulton et al. Mol Ther, 2022). This virus also contained the A56R gene deletion, which reduces virus toxicity and creates a fusogenic phenotype. Since the mechanism of EPAC activation is in part related to viral spread through syncytia, and since we have not determined if it causes cell fusion directly or simply enhances it by improving cell adhesion or cytoskeleton remodeling, we believed it was important to use viruses that caused syncytia naturally. However, we have not fully tested whether this is necessary for all viruses (fusogenic or not) to benefit from EPAC activation. This would be something we would be interested in pursuing further by testing no fusogenic strains of VACV such as Copenhagen as well as other fusogenic and non-fusogenic OVs such as measles and HSV, respectively.

In vivo's with both MC38 IT and IP models showed that TTΔA56R CAT mutant and TTdA56R F300A improved survival relative to WT TTΔA56R . We observed smaller tumors leading to longer survival time with the TTdA56R CAT virus in both IP and IT. WT SKV survival results were not significantly lower than mutants EPAC SKV mutants. We propose this is likely due to the added fusogenic properties of T TTΔA56R and the added persistence in-vivo compared to SKV due to it being less attenuated.

Based on the results from our in vitro and in vivo experiments, we were able to show that the EPAC CAT construct outperformed the other EPAC constructs. EPAC CAT mutation has shown better viral replication, less hindrance from ESI-09 in vitro and greater survival in tumour models. We eliminated 5A earlier while validating expression, since 5A was not able to replicate significantly better than WT SKV. We continued on with CAT and F300A until we saw in MC38 IT, TTΔA56R data that CAT significantly increasing survival compared to F300A so we

pursued CAT. 5A and F300A are both mutations in the helix region that causes the protein to go from inactive to active. While mutating the helix does shift the equilibrium towards open, there is still the possibility of the protein shifting back to inactive. CAT has the regulatory completely removed, thus there is no inactive state to resort to. This could account for the differences we see between the mutants. As well, due to the structure of the 5A, and F300A mutants, there is still a possibility of ES109 inhibiting the mutants, whereas CAT has only the catalytic region, thus no way of being sterically hindered by ESI-09 inhibitor. CAT is also the smallest construct thus allowing most likely for better viral expression.

While our results are still ongoing, another avenue worth perusing would be testing our viruses in more cancer models. It would be worth trying models with high vs low EPAC expression, to see how the viruses respond in both environments. To determine low vs high expression of EPAC in different cancer cell models, we would need to perform gene expression profiling from different tumor tissues to access over expressed vs low expressed genes in a comparative analysis.

6.1 *Future goals*

We plan to preform co-treatment *in vivo*, with virus and ESI-09 drug so we can attack both the tumor and prevent metastases simultaneously. In vitro data shows this is possible. The RAP1 assay we used to show virus replication is less impacted with our mutant EPAC viruses. SKV WT viral replication was hindered when the ESI-09 drug was added causing viral replication to not be more significant than mock. All of the mutant viruses were able to replicate in the presence of ESI-09 and were only slightly hindered. (Fig. 11)

In very preliminary data with the B16 model that we can potentially prevent lung metastases by treating mice, but due to animal guidelines we are required to endpoint the mice

before we see a large number of metastases in untreated mice. It is our goal in the future to surgically remove the primary tumour in our next *in vivo* to allow the cancer to spread for a longer period of time. After which we would be able to resect the lungs and access met spread in treated vs untread mice.

Once we have data showing ES1-09 can prevent tumour metastases, we hope to start using them in combination by treating the tumor initially with virus followed by drug. Optimization will need to be done to determine the most efficient time to administer drug so it does not interfere with virus replication. If limited success is seen with ESI-09 we can attempt other EPAC inhibitors such as CE3F4, I594, or AM-001. (Fig. 9).

Further combination therapies should be investigated, such as a dual viral + drug approach. To date, we have a virus that can over express EPAC without being hindered by ESI-09 . If it can be shown that ESI-09 can reduce tumor metastases and we have shown we can decrease tumor burden with our viruses, we have the potential to introduce a 2nd virus that is designed to specifically target over expressed EPAC, while having no effect on our current viruses by codon optimization. This would allow for a highly specified tumor treatment for tumors over-expressing EPAC, while also inhibiting secondary tumors. (Fig. 12)

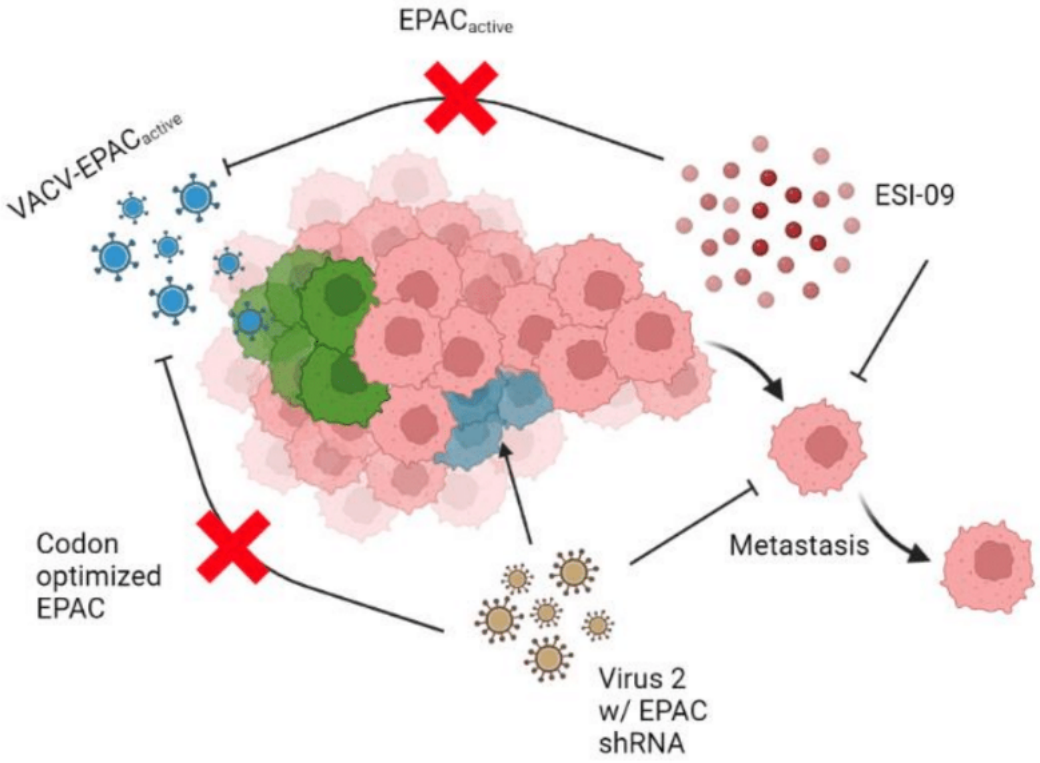

Figure 12. Schematic representation of the combinational therapy of VACV-EPAC viruses with ESI-09. The constitutively active EPAC constructs enhance OV spread in tumors leading to improved efficacy. The EPAC selective inhibitor, ESI-09, blocks cell migration and invasion and acts as an anti-metastatic compound. However, ESI-09 is also a potent inhibitor of virus replication and under normal circumstances would reduce the oncolytic activity of Vaccinia. However, the constitutively active EPAC constructs encoded within our OVs are resistant to ESI-09 and therefore would provide an avenue to combine treatment of oncolytic VACV and ESI-09 together. Another possible strategy to combine the benefits of EPAC activation on OV spread with the anti-metastatic activity of EPAC inhibition is to use short hairpin RNAs (shRNAs) that will knockdown endogenous EPAC, but would be ineffective against EPAC expressed by our viruses due to codon optimization.

6.0 Conclusion

Here, we have designed a virus with TTΔA56R backbone that expressing a constitutively active EPAC and is able to infect and kill cancer cells better than WT TTΔA56R. More research is needed to combine our virus with ESI-09 to create a dual mechanistic oncolytic therapy.

References

1. R. Siegel, D. Naishadham, A. Jemal Cancer statistics 2013, CA Cancer J. Clin., 63 (2013), pp. 11-30
2. C.E. Meacham, S.J. Morrison Tumour heterogeneity and cancer cell plasticity Nature, 501 (2013), pp. 328-337
3. Seyed Hossein Hassanpour, Mohammadamin Dehghani,Review of cancer from perspective of molecular, Journal of Cancer Research and Practice, Volume 4, Issue 4 (2017) pp. 127-129,
4. Zhang S, Rabkin SD. The discovery and development of oncolytic viruses: are they the future of cancer immunotherapy? Expert Opin Drug Discov. 2021 Apr;16(4):391-410
5. Kelly E, Russell SJ. History of oncolytic viruses: genesis to genetic engineering. Mol Ther. 2007 Apr;15(4):651-9.
6. Eggermont AMM, Blank CU, Mandala M, Long GV, Atkinson V, Dalle S, Haydon A, Lichinitser M, Khattak A, Carlino MS, Sandhu S, Larkin J, Puig S, Ascierto PA, Rutkowski P, Schadendorf D, Koornstra R, Hernandez-Aya L, Maio M, van den Eertwegh AJM, Grob JJ, Gutzmer R, Jamal R, Lorigan P, Ibrahim N, Marreaud S, van Akkooi ACJ, Suciu S, Robert C. Adjuvant Pembrolizumab versus Placebo in Resected Stage III Melanoma. N Engl J Med. 2018 May 10;378(19):1789-1801
7. ClinicalTrials.gov
8. Luo-Qin Fu, Shi-Bing Wang, Mao-Hua Cai, Xue-Jun Wang, Jin-Yang Chen, Xiang-Min Tong, Xiao-Yi Chen, Xiao-Zhou Mou. Recent advances in oncolytic virus-based cancer therapy, Virus Research, Volume 270, 2019,197675
9. Kong Yi-chi M., Flynn Jeffrey C. Opportunistic Autoimmune Disorders Potentiated by Immune-Checkpoint Inhibitors Anti-CTLA-4 and Anti-PD-1, Frontiers in Immunology 5, 2014, 1664-3224.
10. Roy Noy, Jeffrey W. Pollard, Tumor-Associated Macrophages: From Mechanisms to Therapy, Immunity, Volume 41, Issue 1, 2014, Pages 49-61,
11. Ahmed, M., McKenzie, M. O., Puckett, S., Hojnacki, M., Poliquin, L., & Lyles, D. S. (2003). Ability of the matrix protein of vesicular stomatitis virus to suppress beta interferon gene expression is genetically correlated with the inhibition of host RNA and protein synthesis. *Journal of virology*, *77*(8), 4646-4657.

12. Pelin, A., Foloppe, J., Petryk, J., Singaravelu, R., Hussein, M., Gossart, F., ... & Bell, J. C. (2019). Deletion of apoptosis inhibitor F1L in vaccinia virus increases safety and oncolysis for cancer therapy. *Molecular Therapy-Oncolytics*, *14*, 246-252.
13. Greseth, M. D., & Traktman, P. (2022). The Life Cycle of the Vaccinia Virus Genome. *Annual Review of Virology*, *9*.
14. Greseth, M. D., & Traktman, P. (2022). The Life Cycle of the Vaccinia Virus Genome. *Annual Review of Virology*, *9*.
15. Pelin, A., Huh, M., Tang, M., LeBouef, F., Keller, B., Duong, J., ... & Bell, J. C. (2020). Abstract PR19: Utilizing novel oncolytic vaccinia virus for selective expression of immunotherapeutic payloads in metastatic tumors. *Cancer Immunology Research*, *8*(4_Supplement), PR19-PR19.
16. Zwiebel, J. A. (2001, August). Cancer gene and oncolytic virus therapy. In *Seminars in oncology* (Vol. 28, No. 4, pp. 336-343). WB Saunders.
17. Bos, J. L. (2003). Epac: a new cAMP target and new avenues in cAMP research. *Nature reviews Molecular cell biology*, *4*(9), 733-738.
18. Cheng, X., Ji, Z., Tsalkova, T., & Mei, F. (2008). Epac and PKA: a tale of two intracellular cAMP receptors. *Acta biochimica et biophysica Sinica*, *40*(7), 651-662.
19. Hoy, J. J., Parra, N. S., Park, J., Kuhn, S., & Iglesias-Bartolome, R. (2020). Protein kinase A inhibitor proteins (PKIs) divert GPCR-Gαs-cAMP signaling towards EPAC and ERK activation and are involved in tumor growth. *FASEB journal: official publication of the Federation of American Societies for Experimental Biology*, *34*(10), 13900.
20. Huff, T. C., Camarena, V., Sant, D. W., Wilkes, Z., Van Booven, D., Aron, A. T., ... & Wang, G. (2020). Oscillatory cAMP signaling rapidly alters H3K4 methylation. *Life science alliance*, *3*(1).
21. Almahariq, M., Chao, C., Mei, F. C., Hellmich, M. R., Patrikeev, I., Motamedi, M., & Cheng, X. (2015). Pharmacological inhibition and genetic knockdown of exchange protein directly activated by cAMP 1 reduce pancreatic cancer metastasis in vivo. *Molecular pharmacology*, *87*(2), 142-149.
22. BOULTON ET AL UNDER REVIEW

23. Li, K., Zhang, H., Qiu, J., Lin, Y., Liang, J., Xiao, X., ... & Yan, G. (2016). Activation of cyclic adenosine monophosphate pathway increases the sensitivity of cancer cells to the oncolytic virus M1. *Molecular Therapy*, *24*(1), 156-165.
24. Almahariq, M., Tsalkova, T., Mei, F. C., Chen, H., Zhou, J., Sastry, S. K., ... & Cheng, X. (2013). A novel EPAC-specific inhibitor suppresses pancreatic cancer cell migration and invasion. *Molecular pharmacology*, *83*(1), 122-128.
25. Rehmann, H., Rueppel, A., Bos, J. L., & Wittinghofer, A. (2003). Communication between the regulatory and the catalytic region of the cAMP-responsive guanine nucleotide exchange factor Epac. *Journal of Biological Chemistry*, *278*(26), 23508-23514.
26. Selvaratnam, R., VanSchouwen, B., Fogolari, F., Mazhab-Jafari, M. T., Das, R., & Melacini, G. (2012). The projection analysis of NMR chemical shifts reveals extended EPAC autoinhibition determinants. *Biophysical journal*, *102*(3), 630-639.
27. O'Shaughnessy, E. C., Stone, O. J., LaFosse, P. K., Azoitei, M. L., Tsygankov, D., Heddleston, J. M., ... & Hahn, K. M. (2019). Software for lattice light-sheet imaging of FRET biosensors, illustrated with a new Rap1 biosensor. *Journal of Cell Biology*, *218*(9), 3153-3160.
28. Tsalkova, T., Mei, F. C., Li, S., Chepurny, O. G., Leech, C. A., Liu, T., ... & Cheng, X. (2012). Isoform-specific antagonists of exchange proteins directly activated by cAMP. *Proceedings of the National Academy of Sciences*, *109*(45), 18613-18618.
29. Chen, H., Ding, C., Wild, C., Liu, H., Wang, T., White, M. A., ... & Zhou, J. (2013). Efficient synthesis of ESI-09, a novel non-cyclic nucleotide EPAC antagonist. *Tetrahedron letters*, *54*(12), 1546-1549.
30. Mucker, E. M., Goff, A. J., Shamblin, J. D., Grosenbach, D. W., Damon, I. K., Mehal, J. M., ... & Hruby, D. E. (2013). Efficacy of tecovirimat (ST-246) in nonhuman primates infected with variola virus (Smallpox). *Antimicrobial agents and chemotherapy*, *57*(12), 6246-6253.
31. 29. Li, Y., Chen, S., Fang, J., Zhu, Y., Bai, B., Li, W., ... & Jin, N. (2018). Construction of an attenuated Tian Tan vaccinia virus strain by deletion of TA35R and TJ2R genes. *Virus research*, *256*, 192-200.
32. https://www2.uottawa.ca/research-innovation/animal-care/ethics-compliance/animal-use-protocol-review-approval

Contributions of Collaborators

Dr. Stephen Boulton provide the preliminary findings figures and data, as well as help with in-vivo studies.

Rida Gill optimized Rap1 assay, as well as purifying TT viruses.

Siddharth Singh performed phalloidin staining.

Mathieu Crupi provided Cell lines involved in paper.

Julia Petryk performed surgery and injections for all mice trials.